Interface-based two-way tuning of the in-plane thermal transport in nanofilms

Yu-Chao Hua and Bing-Yang Cao[a]

Key Laboratory for Thermal Science and Power Engineering of Ministry of Education, Department of Engineering Mechanics, Tsinghua University, Beijing 100084, China

Here, the two-way tuning of in-plane thermal transport is obtained in the bi-layer nanofilms with an interfacial effect by using the Boltzmann transport equation (BTE) and the phonon Monte Carlo (MC) technique. A thermal conductivity model was derived from the BTE and verified by the MC simulations. Both the model and the MC simulations indicate that the tuning of the thermal transport can be bidirectional (reduced or enhanced), depending on the interface conditions (i.e., roughness and adhesion energy) and the phonon property dissimilarity at the interface. For the identical-material interface, the emergence of thermal conductivity variation requires two conditions: (a) the interface is not completely specular and (b) the transmission specularity parameter differs from the reflection specularity parameter at the interface. When the transmission specularity parameter is larger than the reflection specularity parameter at the interface, the thermal conductivity improvement effect emerges, whereas the thermal conductivity reduction effect occurs. For the disparate-material interface, the phonon property perturbation near the interface causes the thermal conductivity variation, even when neither the above two conditions are satisfied. The mean free path ratio (γ) between the disparate materials was defined to characterize the phonon property dissimilarity. $\gamma > 1$ can lead to the thermal conductivity improvement effect, while $\gamma < 1$ corresponds to the thermal conductivity reduction effect. Our work provides a more in-depth understanding of the interfacial effect on the nanoscale thermal transport, with an applicable predictive model, which can be helpful for predicting and manipulating phonon transport in nanofilms. *Published by AIP Publishing.* https://doi.org/10.1063/1.5013657

I. INTRODUCTION

With the rapid development of fabrication technologies, the density of interfaces keeps increasing within electronic micro/nano-devices.[1,2] The interface has significant impacts on thermal transport in electronic devices,[3–7] and importantly it can be used to effectively tune the thermal properties of nanomaterials.[8–17] In the direction normal to the interface (the cross-plane direction), it can introduce a thermal resistance and degrade the thermal transport ability.[18–21] Two limiting models[18] have been long-termly used to calculate the interface resistance, i.e., the acoustic mismatch model (AMM), which assumes no scattering, and the diffuse mismatch model (DMM), which assumes that the phonons striking at the interface will diffusively scatter. Then, Prasher[19] modified the AMM to involve the influence of the van der Waals (vdW) contacts. Recently, the time-domain thermoreflectance (TDTR) experiments by Wilson and Cahill[20] show that the interfacial resistance becomes dependent on the phonon mean free path (MFP) in the ballistic-diffusive regime, due to the interface-ballistic coupling effect. Moreover, Hua and Cao[21] studied the boundary temperature jumps, and proposed a model that concerns both the interfacial resistance and the ballistic effect.

In fact, the interface also significantly affects the in-plane thermal transport process. This point has been investigated particularly for single-layer and multiple-layer two-dimensional materials.[22–26] For example, the in-plane thermal conductivity of the supported graphene is lower than that of the suspended one, which has been attributed to the interlayer phonon scattering.[23,24] However, the experiments of Yang *et al.*[27] demonstrated that a vdW interface between two nanoribbons made of identical materials could improve the thermal conductivity parallel to the interface (i.e., the in-plane thermal conductivity). A semi-quantitative model was proposed to explain the experimental data. This model merely highlights the influence of interface adhesion energy that determines the phonon transmissivity through the interface. Then, Guo *et al.*[28] calculated the thermal conductivity of a one-dimensional (1D) chain on the substrate (the other 1D chain), and also found that in certain regions the coupling to substrates can improve the thermal conductivity. Similarly, Sun *et al.*[29] performed molecular dynamics (MD) simulations in a system of two 1D chains with vdW interactions between them, and concluded that whether the thermal conductivity is enhanced depending on the intensity of vdW interactions. In the case of moderate vdW interactions, the thermal conductivity could be reduced, while in the case of strong vdW interactions the thermal conductivity could be enhanced. Moreover, this 1D model was also studied by Su *et al.*[30] through MD simulations, and the authors concluded that the thermal transport improvement effect should be attributed to the nonlinear interface interaction. In fact, the simulation

---

a)Author to whom correspondence should be addressed: caoby@tsinghua.edu.cn

models of Guo et al.,[28] Sun et al.,[29] and Su et al.[30] could be a little bit oversimplified, and thus, some other important factors, such as interface roughness, had not been well addressed. By contrast, through running MD simulations, Chen et al.[31] found that interface roughness is also a critical factor in this case: an atomically smooth interface will lead to the same in-plane thermal conductivity of a bi-layer film as that of a single layer, while the thermal conductivity improvement effect could occur as roughness is introduced at the interface.

Additionally, an interface usually exists between two disparate materials in practice, that is to say, the effects of phonon property dissimilarity also have an impact on the thermal transport, which were not concerned in the phenomenological model by Yang et al.[27] or Chen et al.[31] By using MD simulations, Zhang et al.[32] found that the thermal conductivity of silicene on the substrate could be either enhanced or suppressed by changing the property of the substrate. Indeed, it could still be an open question whether the thermal transport improvement by the interface can be achieved even in the case with phonon property dissimilarity at the interface. Moreover, due to the absence of a unified and rigorous analysis model, even for the thermal transport in the supported graphene that has been extensively studied, some issues are still in debate. For example, MD simulation results by Ong et al.[23] show that the thermal conductivity of a supported graphene could be enhanced with the increasing strength of coupling between graphene and substrate; however, Qiu and Ruan[24] obtained a contrary conclusion that stronger interfacial bonding results in more thermal conductivity reduction.

The interface-based tuning of the thermal transport should depend on three major factors: (a) interface adhesion energy, (b) interface roughness, and (c) phonon property dissimilarity. In the present work, we focus on the interfacial effect on the in-plane thermal transport in the nanofilms. An analytical thermal conductivity model that concerns the three factors above was derived based on the phonon Boltzmann transport equation (BTE). For verification, a phonon Monte Carlo (MC) technique was used to simulate the phonon transport process. The two-way tuning of the in-plane thermal transport was identified, that is to say, an interface can reduce or enhance the in-plane thermal conductivity, depending on the interface conditions and the phonon property dissimilarity at the interface.

II. MODEL DERIVATION

A. In-plane thermal conductivity of suspended nanofilms

Figure 1(a) shows a suspended nanofilm with the reflection specularity parameters equal to P_{r1} and P_{r2}, respectively. In this case, the lateral boundaries are adiabatic, and thus, all the phonons striking on them will be reflected back. The reflection specularity parameters, P_{r1} and P_{r2}, should depend on the boundary roughness,[33,34] that is, $P_{r1(2)} = \exp\left(-16\pi^2\Delta^2/\lambda^2\right)$, in which Δ is the root-mean-square value of the roughness fluctuations and λ is the phonon wavelength. We assume that the length in the heat flow direction is much longer than the phonon MFP, while the lateral width (L_y) is comparable to the phonon MFP. The corresponding phonon BTE is given by[33]

$$v_{g\omega y}\tau_\omega \frac{\partial \Delta f_\omega}{\partial y} + \Delta f_\omega = -v_{g\omega x}\tau_\omega \frac{\partial f_{0\omega}}{\partial T}\frac{dT}{dx} \qquad (1)$$

with the boundary conditions

$$\begin{aligned}
\Delta f_\omega(0, v_{g\omega y} > 0) &= P_{r1}\Delta f_\omega(0, v_{g\omega y} < 0), \\
\Delta f_\omega(L_y, v_{g\omega y} < 0) &= P_{r2}\Delta f_\omega(L_y, v_{g\omega y} > 0),
\end{aligned} \qquad (2)$$

where ω is the angular frequency, $v_{g\omega y}$ is the group velocity, f_ω is the phonon distribution function, $f_{0\omega}$ is the equilibrium distribution function, and τ_ω is the relaxation time, and $\Delta f_\omega = f_\omega - f_{0\omega}$. Combination of Eqs. (1) and (2) gives the heat flux

$$q_x(y) = \frac{dT}{dx}\int_0^{\omega_m} \frac{v_{g\omega}l_{0\omega}}{4}\omega\hbar\frac{\partial f_{BE}}{\partial T}D(\omega)d\omega$$

$$\times\left[\int_0^1\left(G^+ \exp\left(-\frac{y}{l_{0\omega}\mu}\right)\right)(1-\mu^2)d\mu\right.$$

$$\left.+\int_0^1\left(G^- \exp\left(\frac{y}{l_{0\omega}\mu}\right)\right)(1-\mu^2)d\mu - \frac{4}{3}\right] \qquad (3)$$

with

$$G^+ = \frac{1 - P_{r2}\left[1 - (1-P_{r1})\exp\left(-\frac{L_y}{l_{0\omega}\mu}\right)\right]}{1 - P_{r1}P_{r2}\exp\left(-2\frac{L_y}{l_{0\omega}\mu}\right)}$$
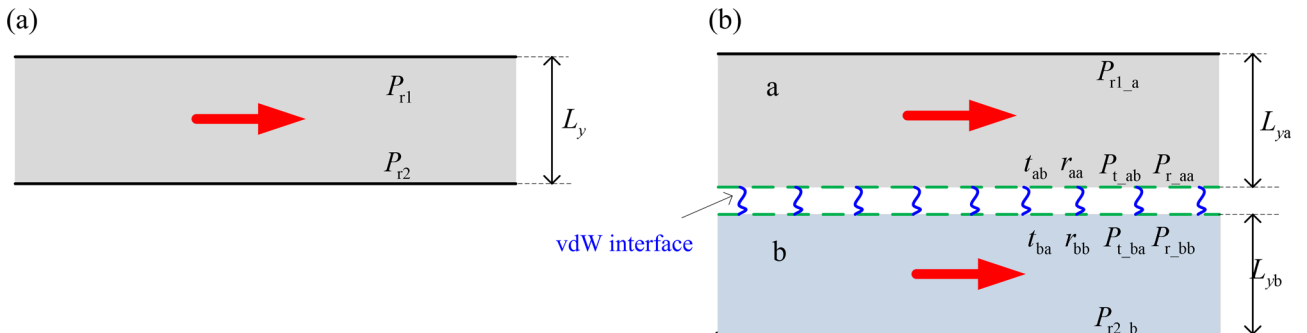

FIG. 1. (a) Schematic of a typical suspended nanofilm; (b) schematic of a typical bi-layer nanofilm with a vdW interface.

and

$$G^- = \exp\left(-\frac{L_y}{l_{0\omega}\mu}\right) \frac{1 - P_{r1}\left[1 - (1 - P_{r2})\exp\left(-\frac{L_y}{l_{0\omega}\mu}\right)\right]}{1 - P_{r1}P_{r2}\exp\left(-2\frac{L_y}{l_{0\omega}\mu}\right)}$$

in which ω_m is the cutoff angular frequency, f_{BE} is Bose-Einstein distribution, $\hbar$ is the Dirac constant, $D(\omega)$ is the density of states, $l_{0\omega} = v_{g\omega}\tau_\omega$ is the intrinsic phonon MFP, and $\mu = \cos(\theta)$, where θ is the polar angle. Using the Fourier's law, we can derive the in-plane thermal conductivity of this suspended nanofilm

$$
\begin{aligned}
k_{eff} &= -\frac{1}{(dT/dx)L_y}\int_0^{L_y} q_x(y)dy \\
&= \frac{1}{3L_y}\int_0^{\omega_m} v_{g\omega}l_{0\omega}\omega\hbar\frac{\partial f_{BE}}{\partial T}D(\omega)d\omega \\
&\times \int_0^{L_y}\left[1 - \frac{3}{4}\int_0^1\left(G^+\exp\left(-\frac{y}{l_{0\omega}\mu}\right)\right.\right. \\
&\left.\left. + G^-\exp\left(\frac{y}{l_{0\omega}\mu}\right)\right)(1-\mu^2)d\mu\right]dy.
\end{aligned}
\tag{4}
$$

This model is a minor extension of the widely used Fuchs-Sondheimer formula.[35–38] Malhotra et al.[39] also derived this model. In the present work, it is used to give some benchmarked results to verify our MC simulations and to compare with the results involving the interfacial effect.

B. In-plane thermal conductivity of nanofilms with the interface

In this section, we turn to the case with the interfacial effect. Figure 1(b) shows a bi-layer nanofilm with an interface. A vdW interface is between these two layers. The phonons in layer "a" can scatter on the interface, or pass through the interface and enter layer "b". The phonons in layer "b" also undergo the identical process.

The phonon BTEs for the layers labelled by "a" and "b" are given by

$$v_{g\omega y\_a}\tau_{\omega\_a}\frac{\partial\Delta f_{\omega\_a}}{\partial y} + \Delta f_{\omega\_a} = -v_{g\omega x\_a}\tau_{\omega\_a}\frac{\partial f_{\omega0\_a}}{\partial T}\frac{dT}{dx} \tag{5}$$

and

$$v_{g\omega y\_b}\tau_{\omega\_b}\frac{\partial\Delta f_{\omega\_b}}{\partial y} + \Delta f_{\omega\_b} = -v_{g\omega x\_b}\tau_{\omega\_b}\frac{\partial f_{\omega0\_b}}{\partial T}\frac{dT}{dx} \tag{6}$$

with the interface and boundary conditions

$$
\begin{aligned}
\Delta f_{\omega\_a}(L_{ya}, v_{g\omega y\_a} < 0) &= P_{r1\_a}\Delta f_{\omega\_a}(L_{ya}, v_{g\omega y\_a} > 0); \\
\Delta f_{\omega a}(0, v_{g\omega y\_a} > 0) &= P_{r\_aa}r_{aa}\Delta f_{\omega\_a}(0, v_{g\omega y\_a} < 0) + P_{t\_ba}t_{ba}\Delta f_{\omega\_b}(0, v_{g\omega y\_b} > 0), \\
\Delta f_{\omega b}(0, v_{g\omega y\_b} < 0) &= P_{r\_bb}r_{bb}\Delta f_{\omega\_b}(0, v_{g\omega y\_b} > 0) + P_{t\_ab}t_{ab}\Delta f_{\omega\_a}(0, v_{g\omega y\_a} < 0); \\
\Delta f_{\omega\_b}(-L_{yb}, v_{g\omega y\_b} > 0) &= P_{r2\_b}\Delta f_{\omega\_b}(L_{ya}, v_{g\omega y\_b} < 0).
\end{aligned}
\tag{7}
$$

In Eq. (7), in order to describe the phonon transmission and reflection probabilities at the interface, two transmissivities (t_{ab}, t_{ba}) as well as the two corresponding reflectivities (r_{aa}, r_{bb}) were introduced, and $t_{ab} = 1 - r_{aa}$, $t_{ba} = 1 - r_{bb}$. According to the phonon transmissivity model by Prasher,[19] the influence of the vdW interaction strength (or the interface adhesion energy) can be involved in the phonon transmissivity. Moreover, four reflection specularity parameters (P_{r1_a}, P_{r_aa}, P_{r_bb}, and P_{r2_b}) are used to describe the phonon reflection mode (specularly or diffusively) at the boundaries and the interface. According to Ref. 40, at the interface, the specularity parameter of the transmitted phonons can differ from that of the reflected phonons, and this view can be supported by the experiments by Yang et al.[27] Thus, two transmission specularity parameters (P_{t_ab}, P_{t_ba}) are introduced to characterize the phonon transmission mode through the interface.

Then, combining Eqs. (5)–(7), we can have

$$
\begin{aligned}
0 \le y < L_{ya}: q_{xa}(y) &= \frac{dT}{dx}\int_0^{\omega_{ma}}\frac{v_{ga}l_{0\omega a}}{4}\omega\hbar\frac{\partial f_{BE}}{\partial T}D(\omega)d\omega \\
&\times\left[\int_0^1\left(G_a^+\exp\left(-\frac{y}{l_{0\omega a}\mu}\right)\right)(1-\mu^2)d\mu + \int_0^1\left(G_a^-\exp\left(\frac{y}{l_{0\omega a}\mu}\right)\right)(1-\mu^2)d\mu - \frac{4}{3}\right]
\end{aligned}
\tag{8}
$$

and

$$
\begin{aligned}
-L_{yb} \le y < 0: q_{xb}(y) &= \frac{dT}{dx}\int_0^{\omega_{mb}}\frac{v_{gb}l_{\omega0b}}{4}\omega\hbar\frac{\partial f_{BE}}{\partial T}D(\omega)d\omega \\
&\times\left[\int_0^1\left(G_b^+\exp\left(-\frac{y}{l_{\omega0b}\mu}\right)\right)(1-\mu^2)d\mu + \int_0^1\left(G_b^-\exp\left(\frac{y}{l_{\omega0b}\mu}\right)\right)(1-\mu^2)d\mu - \frac{4}{3}\right]
\end{aligned}
\tag{9}
$$

with

$$G_a^+=\frac{\left\{\begin{array}{l}(1-P_{r1\_a})P_{r\_aa}r_{aa}\exp\left(-\dfrac{L_{ya}}{l_{0\omega a}\mu}\right)+\exp\left(-\dfrac{L_{yb}}{l_{0\omega b}\mu}\right)\gamma(1-P_{r2\_b})P_{t\_ba}t_{ba}+(1-P_{r\_aa}r_{aa}-\gamma P_{t\_ba}t_{ba})\\[2mm]-(1-P_{r1\_a})P_{r2\_b}(P_{r\_aa}P_{r\_bb}r_{aa}r_{bb}-P_{t\_ab}P_{t\_ba}t_{ab}t_{ba})\exp\left(-2\dfrac{L_{yb}}{l_{0\omega b}\mu}-\dfrac{L_{ya}}{l_{0\omega a}\mu}\right)\\[2mm]+\exp\left(-2\dfrac{L_{yb}}{l_{0\omega b}\mu}\right)P_{r2\_b}(\gamma P_{t\_ba}t_{ba}-P_{r\_bb}r_{bb}+P_{r\_aa}P_{r\_bb}r_{aa}r_{bb}-P_{t\_ab}P_{t\_ba}t_{ab}t_{ba})\end{array}\right\}}{1-\exp\left(-\dfrac{2L_{ya}}{l_{0\omega a}\mu}\right)P_{r1\_a}P_{r\_aa}r_{aa}-\exp\left(-\dfrac{2L_{yb}}{l_{0\omega b}\mu}\right)P_{r2\_b}P_{r\_bb}r_{bb}+P_{r1\_a}P_{r2\_b}(P_{r\_aa}P_{r\_bb}r_{aa}r_{bb}-P_{t\_ab}P_{t\_ba}t_{ab}t_{ba})\exp\left(-\dfrac{2L_{ya}}{l_{0\omega a}\mu}-\dfrac{2L_{yb}}{l_{0\omega b}\mu}\right)},$$

$$G_a^-=\frac{\exp\left(-\dfrac{L_{ya}}{l_{0\omega a}\mu}\right)\left\{\begin{array}{l}(1-P_{r1\_a})-\exp\left(-2\dfrac{L_{yb}}{l_{0\omega b}\mu}\right)(1-P_{r1\_a})P_{r2\_b}P_{r\_bb}r_{bb}+\exp\left(-\dfrac{L_{ya}}{l_{0\omega a}\mu}-\dfrac{L_{yb}}{l_{0\omega b}\mu}\right)\gamma P_{r1\_a}(1-P_{r2\_b})P_{t\_ba}t_{ba}\\[2mm]+\exp\left(-\dfrac{L_{ya}}{l_{0\omega a}\mu}-2\dfrac{L_{yb}}{l_{0\omega b}\mu}\right)P_{r1\_a}P_{r2\_b}(\gamma P_{t\_ba}t_{ba}-P_{r\_bb}r_{bb}+P_{r\_bb}P_{r\_aa}r_{aa}r_{bb}-P_{t\_ab}P_{t\_ba}t_{ab}t_{ba})\\[2mm]+\exp\left(-\dfrac{L_{ya}}{l_{0\omega a}\mu}\right)P_{r1\_a}(1-P_{r\_aa}r_{aa}-\gamma P_{t\_ba}t_{ba})\end{array}\right\}}{1-\exp\left(-\dfrac{2L_{ya}}{l_{0\omega a}\mu}\right)P_{r\_a}P_{r\_aa}r_{aa}-\exp\left(-\dfrac{2L_{yb}}{l_{0\omega b}\mu}\right)P_{r2\_b}P_{r\_bb}r_{bb}+P_{r1\_a}P_{r2\_b}(P_{r\_aa}P_{r\_bb}r_{aa}r_{bb}-P_{t\_ab}P_{t\_ba}t_{ab}t_{ba})\exp\left(-\dfrac{2L_{ya}}{l_{0\omega a}\mu}-\dfrac{2L_{yb}}{l_{0\omega b}\mu}\right)},$$

$$G_b^+=\frac{\exp\left(-\dfrac{L_{yb}}{l_{0\omega b}\mu}\right)\left\{\begin{array}{l}(1-P_{r2\_b})-\exp\left(-2\dfrac{L_{ya}}{l_{0\omega a}\mu}\right)P_{r1\_a}P_{r\_aa}(1-P_{r2\_b})r_{aa}+\exp\left(-\dfrac{L_{ya}}{l_{0\omega a}\mu}-\dfrac{L_{yb}}{l_{0\omega b}\mu}\right)\gamma^{-1}(1-P_{r1\_a})P_{r2\_b}P_{t\_ab}t_{ab}\\[2mm]+P_{r1\_a}P_{r2\_b}(\gamma^{-1}P_{t\_ab}t_{ab}-P_{r\_aa}r_{aa}+P_{r\_aa}P_{r\_bb}r_{aa}r_{bb}-P_{t\_ab}P_{t\_ba}t_{ab}t_{ba})\exp\left(-2\dfrac{L_{ya}}{l_{0\omega a}\mu}-\dfrac{L_{yb}}{l_{0\omega b}\mu}\right)\\[2mm]+\exp\left(-\dfrac{L_{yb}}{l_{0\omega b}\mu}\right)P_{r2\_b}(1-P_{r\_bb}r_{bb}-\gamma^{-1}P_{t\_ab}t_{ab})\end{array}\right\}}{1-\exp\left(-\dfrac{2L_{ya}}{l_{0\omega a}\mu}\right)P_{r1\_a}P_{r\_aa}r_{aa}-\exp\left(-\dfrac{2L_{yb}}{l_{0\omega b}\mu}\right)P_{r2\_b}P_{r\_bb}r_{bb}+P_{r1\_a}P_{r2\_b}(P_{r\_aa}P_{r\_bb}r_{aa}r_{bb}-P_{t\_ab}P_{t\_ba}t_{ab}t_{ba})\exp\left(-\dfrac{2L_{ya}}{l_{0\omega a}\mu}-\dfrac{2L_{yb}}{l_{0\omega b}\mu}\right)},$$

$$G_b^-=\frac{\left\{\begin{array}{l}\exp\left(-\dfrac{L_{yb}}{l_{0\omega b}\mu}\right)(1-P_{r2\_b})P_{r\_bb}r_{bb}+\exp\left(-\dfrac{L_{ya}}{l_{0\omega a}\mu}\right)\gamma^{-1}(1-P_{r1\_a})P_{t\_ab}t_{ab}+(1-P_{r\_bb}r_{bb}-\gamma^{-1}P_{t\_ab}t_{ab})\\[2mm]-P_{r1\_a}(1-P_{r2\_b})(P_{r\_aa}P_{r\_bb}r_{aa}r_{bb}-P_{t\_ab}P_{t\_ba}t_{ab}t_{ba})\exp\left(-2\dfrac{L_{ya}}{l_{0\omega a}\mu}-\dfrac{L_{yb}}{l_{0\omega b}\mu}\right)\\[2mm]+\exp\left(-2\dfrac{L_{ya}}{l_{0\omega a}\mu}\right)P_{r1\_a}(\gamma^{-1}P_{t\_ab}t_{ab}-P_{r\_ab}r_{aa}+P_{r\_aa}P_{r\_bb}r_{aa}r_{bb}-P_{t\_ab}P_{t\_ba}t_{ab}t_{ba})\end{array}\right\}}{1-\exp\left(-\dfrac{2L_{ya}}{l_{0\omega a}\mu}\right)P_{r\_a}P_{r\_aa}r_{aa}-\exp\left(-\dfrac{2L_{yb}}{l_{0\omega b}\mu}\right)P_{r\_b}P_{r\_bb}r_{bb}+P_{r1\_a}P_{r2\_b}(P_{r\_aa}P_{r\_bb}r_{aa}r_{bb}-P_{t\_ab}P_{t\_ba}t_{ab}t_{ba})\exp\left(-\dfrac{2L_{ya}}{l_{0\omega a}\mu}-\dfrac{2L_{yb}}{l_{0\omega b}\mu}\right)},$$

where $\gamma=l_{0\omega b}/l_{0\omega a}$ is the MFP ratio. Therefore, the in-plane thermal conductivity models for the layers "a" and "b" are given by

$$
\begin{aligned}
k_{\text{eff\_a}}&=-\frac{1}{(dT/dx)L_{ya}}\int_0^{L_{ya}}q_{xa}(y)dy\\[2mm]
&=\frac{1}{3L_{ya}}\int_0^{\omega_{ma}}v_{g\omega\_a}l_{0\omega a}\omega\hbar\frac{\partial f_{BE}}{\partial T}D(\omega)d\omega\int_0^{L_{ya}}\left[1-\frac{3}{4}\int_0^1\left(G_a^+\exp\left(-\frac{y}{l_{0\omega a}\mu}\right)+G_a^-\exp\left(\frac{y}{l_{0\omega a}\mu}\right)\right)(1-\mu^2)d\mu\right]dy,
\end{aligned}
\tag{10}
$$

and

$$
\begin{aligned}
k_{\text{eff\_b}}&=-\frac{1}{(dT/dx)L_{yb}}\int_0^{L_{yb}}q_{xb}(y)dy\\[2mm]
&=\frac{1}{3L_{ya}}\int_0^{\omega_{mb}}v_{g\omega\_b}l_{0\omega b}\omega\hbar\frac{\partial f_{BE}}{\partial T}D(\omega)d\omega\int_0^{L_{yb}}\left[1-\frac{3}{4}\int_0^1\left(G_b^+\exp\left(-\frac{y}{l_{0\omega b}\mu}\right)+G_b^-\exp\left(\frac{y}{l_{0\omega b}\mu}\right)\right)(1-\mu^2)d\mu\right]dy.
\end{aligned}
\tag{11}
$$

Owing to the interface, the model here becomes much more complicated when compared to that of the suspended nanofilms. Actually, Hua and Cao[21] derived an in-plane thermal conductivity model for the nanofilms on the substrate. However, that model is relatively simple and involves some simplifications on the boundary conditions of the substrate. It cannot concern the disparity between the reflection and the transmission specularity parameters which plays an important role in the two-way tuning of in-plane thermal transport in nanofilms. The present model is an important improvement of the Fuchs-Sondheimer formula. The interface parameters within the model depend on the interface conditions. In general, the values of specularity parameters can increase with the decreasing interface roughness.[33] According to the literature by Li and McGaughey,[40] the reflection specularity parameter is usually smaller than the transmission specularity parameter at the interface. The phonon transmissivity is determined by both the vdW interaction strength and the phonon property mismatch at the interface. Referring to the modified acoustic mismatch model by Prasher,[19] the increasing vdW interaction strength can enhance the phonon transmissivity, while the mismatch of phonon properties will impede phonon transmission through the interface. Therefore, in practice, the in-plane thermal transport can be effectively tuned by changing the interface conditions. For example, in the experiments by Yang *et al.*,[41] the authors demonstrated that the interface conditions (including the thickness of a-SiO$_2$ and the bond types at the interface) can be modified to tune the in-plane thermal transport within the bi-layer nanofilms.

III. PHONON MONTE CARLO TECHNIQUE

We also used a phonon MC technique[42–46] to simulate the phonon transport in the nanofilms. It simulates the phonon transport process by random number samplings.[43] In principle, the phonon MC simulation includes six steps as follows:

(1) *Initialization*: Input the phonon properties (such as MFPs, group velocities, etc.).
(2) *Phonon bundle emission*: Draw the initial properties (including the initial position and traveling direction) of a phonon bundle by random number samplings, according to the nature of the emitting boundary.
(3) *Phonon bundle moving*: Calculate the traveling length until the first scattering event and renew the position of the phonons bundle.
(4) *Interaction with boundary (interface)*: When a phonon bundle collides with a boundary (or an interface), renew the phonon bundle position, and then a random number sampling is conducted to determine whether the phonon bundle can be transmitted; if the phonon bundle is transmitted, a random number sampling is conducted to determine the transmission mode (diffusively or specularly), whereas the phonon bundle is reflected, and a random number sampling is then conducted to determine the reflection mode (diffusively or specularly);
(5) *Phonon bundle reemission*: If a phonon bundle does not collide with any boundary or interface, the phonon

bundle should reemit at the place where the internal scattering event occurs; then, we proceed to (3).
(6) *Phonon bundle tracing termination*: If the phonon bundle arrives at the absorbing boundaries,[44] the tracing process of this phonon bundle is finished; we then proceed to (2) and begin the tracing of the next phonon bundle.

The phonon MC technique has been successfully employed to characterize the thermal transport in various nanostructures, including nanofilms,[42] nanowires,[43,44] and nanoporous structures,[45,46] etc. In fact, this simulation technique is equivalent to numerically solving the phonon Boltzmann transport equation (BTE) which has been widely used to handle the phonon transport problems. Therefore, we chose the MC simulation results as the benchmark to verify our analytical model derived from the phonon BTE. For the suspended nanofilms, the simulation details are similar to those we presented in Ref. 44. Particularly for the bi-layer nanofilms with the interface, the key point is to deal with the phonon-interface interactions. In fact, the algorithm of the random number samplings that handle the phonon-interface interactions, including reflection and transmission at the interface, is the same as that in the previous papers.[44,45] Importantly, in the present work, the MC simulations must be able to consider the disparity between the reflection and the transmission specularity parameters at the interface. Therefore, in our simulations, when a phonon bundle arrives at the interface, the specularity parameter in the random number sampling for determining the reflection mode can be different from that for determining the transmission mode.

IV. RESULTS AND DISCUSSION

A. Interface between the identical materials

We begin by analyzing the thermal transport in the nanofilms with the interface between the identical materials. The two layers "a" and "b" are identical and both made of crystalline silicon. Debye approximation is adopted, and referring to Chen's work,[47] we have $k_0 = 142$ W/mK, $C_V = 0.93 \times 10^6$ J/m^{3}K, $\rho = 2330$ kg/m^3, $v_g = 1804$ m/s, and MFP = 260.4 nm. Since the layers "a" and "b" are identical, we have $P_{r1\_a} = P_{r2\_b}$, $P_{r\_aa} = P_{r\_bb}$, $P_{t\_aa} = P_{t\_bb}$, $t_{ab} = t_{ba}$, $r_{aa} = r_{bb}$, and $k_{eff\_a} = k_{eff\_b}$. Kn is the Knudsen number, with $Kn = \text{MFP}/L_y$ for the suspended nanofilms and $Kn = \text{MFP}/L_{ya}$ for the bi-layer nanofilms. It is noted that the Debye approximation and the bulk-dispersion-based average phonon properties are adopted in the numerical experiments for simplicity. Since the parameter settings in the model are identical to those in the MC simulations, their agreements can prove the model's validity. In fact, with the thickness decreasing, the phonon dispersions will change, which can also influence the thermal conductivity.[34] Our model derivation in Sec. II will not be affected by the choice of the phonon MFPs and group velocities. Referring to Eq. (10), when the phonon properties that concern the phonon dispersion changes are adopted in the model, it can be used to calculate the thermal conductivity involving the influence of phonon dispersion changes.
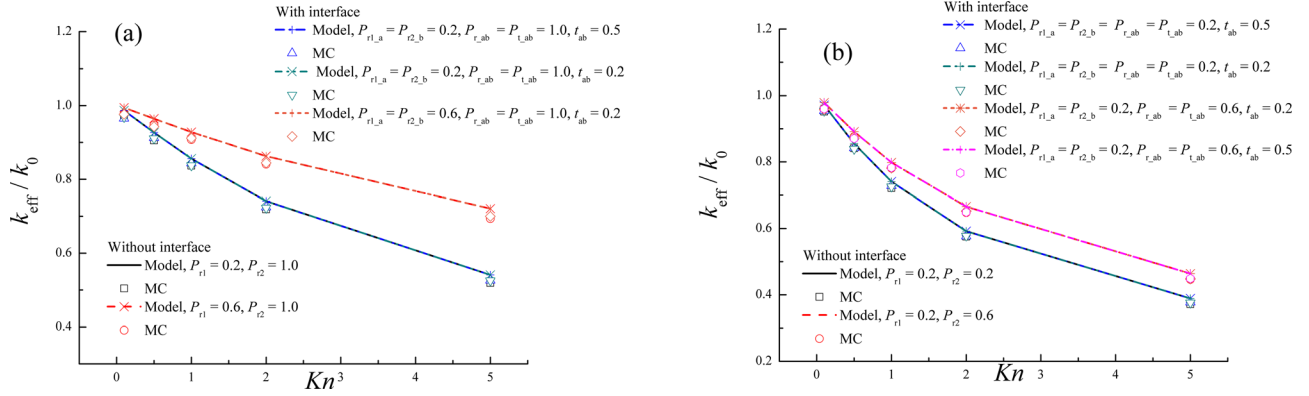
FIG. 2. (a) In-plane thermal conductivity of nanofilms with the completely specular interface between the identical materials, in comparison to that without the interfacial effect; (b) in-plane thermal conductivity of nanofilms with the partially specular interface between the identical materials, and the transmission specularity parameter is set equal to the reflection specularity parameter at the interface.

Figure 2(a) illustrates the in-plane thermal conductivity of the nanofilms with the completely specular interface between the identical materials. Also, the in-plane thermal conductivity of the suspended nanofilms was calculated for comparison. The completely specular interface corresponds to the atomically smooth interface; thus, the transmission and the reflection specularity parameters at the interface are both equal to 1 in this case. As shown in Fig. 2(a), the good agreements between the MC simulations and our model are achieved (their deviations can be less than 10%), verifying the validity of our present models. Moreover, both the MC simulations and the model indicate that a completely specular interface can lead to the same in-plane thermal conductivity of a bi-layer film as that of a single layer one, despite the film thickness and the phonon transmissivity. This conclusion was also obtained in the MD simulations by Chen *et al.*,[31] and now it is re-confirmed via our model and simulations. In the in-plane nanofilms, the completely specular interface will not change the lateral component of the direction vector of the phonons striking on it; therefore, it will have no influence on the in-plane thermal transport. As evidence, the variation of the transmissivity does not cause the variation of the in-plane thermal conductivity in this case. In fact, as shown in Fig. 2(b), even a partially specular interface cannot lead to the thermal conductivity improvement effect, once the reflection specularity parameter is equal to the transmission specularity parameter at the interface. When phonons arrive at the interface, since the reflection and transmission specularity parameters are identical, the transmitted phonons will hold the same possibility to become diffusive as with the reflected phonons, that is to say, the interface is just equivalent to a purely reflective boundary in this case. Then, the characteristic thickness of the bi-layer nanofilms should be identical to that of the one-layer nanofilms. Therefore, both the model and the simulations show that the in-plane thermal conductivity of the bi-layer nanofilms is the same as that of the suspended one-layer nanofilms. The variation of phonon transmissivity through the interface cannot cause the in-plane thermal conductivity variation, either, in this case. In the paper by Li and McGaughey,[40] this point was also emphasized to

explain the in-plane thermal conductivity improvement phenomenon in the experiments by Yang *et al.*[27]

To observe the thermal conductivity variation caused by the interfacial effect, the transmission specularity parameter should be set different from the reflection specularity parameter at the interface. In Fig. 3, the reflection specularity parameter at the interface is 0.2, while the transmission specularity parameter is 1. The phonons will ballistically pass through the interface. Both the MC simulations and the model indicate that the thermal conductivity improvement effect occurs: the in-plane thermal conductivity of the bi-layer nanofilms with the interfacial effect becomes higher than that of the suspended nanofilms, and the thermal conductivity improvement effect is enhanced with the increasing transmissivity. The interface can provide coupling between two layers. In an extreme case with phonon transmissivity equal to unity, phonons will ballistically transmit through it without undergoing any scattering. Then, the bi-layer film is nothing but a single film of double thickness. Owing to the increasing thickness, the strength of boundary scattering degrades and thus, the thermal conductivity increases. Although the phonon transmissivity through the interface
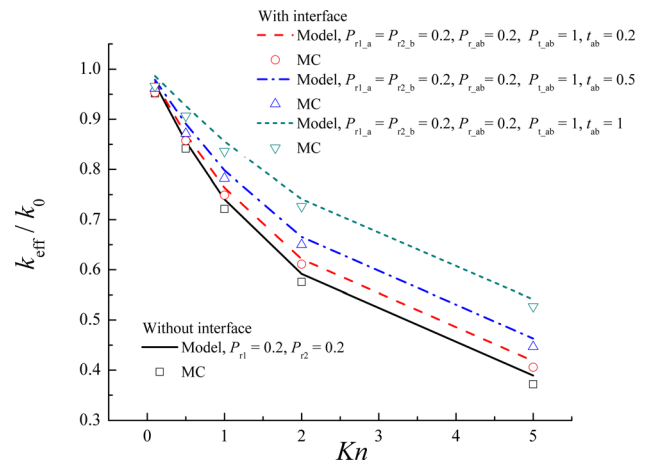

FIG. 3. In-plane thermal conductivity of nanofilms with the partially specular interface between the identical materials, in comparison to that without the interfacial effect. The transmission specularity parameter is different from the reflection specularity parameter at the interface, and the transmission coefficients are 0.2, 0.5, and 1, respectively.
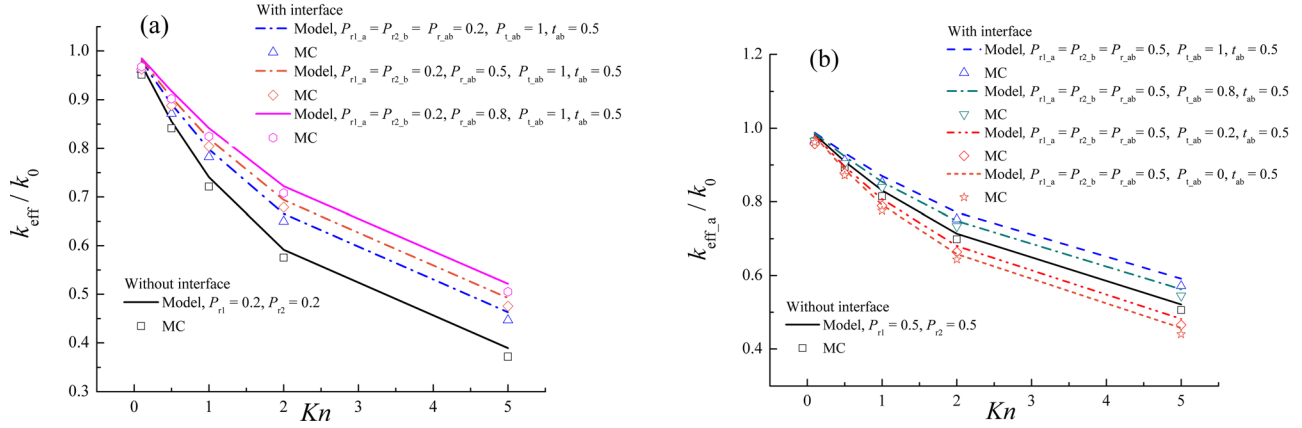
FIG. 4. In-plane thermal conductivity of nanofilms with the partially specular interface between the identical materials, and the transmission specularity parameters are different from the reflection specularity parameters at the interface. (a) The reflection specularity parameters at the interface are 0.2, 0.5, and 0.8, respectively; (b) the transmission specularity parameters at the interface are 0, 0.2, 0.8, and 1, respectively.

may not reach unity, the coupling between two layers can enhance the thermal conductivity on some level.

In Fig. 4(a), the transmission specularity parameter and the transmissivity are given, while the reflection specularity parameters at the interface are set as 0.2, 0.5, and 0.8, respectively. When the phonons can ballistically pass through the interface, the thermal conductivity improvement effect is enhanced with the increasing reflection specularity parameter at the interface. In Fig. 4(b), the reflection specularity parameters are 0.5, the transmissivity is 0.5, and the transmission specularity parameters at the interface are set as 0, 0.2, 0.8, and 1, respectively. As the transmission specularity parameter is larger than the reflection specularity parameter, the thermal conductivity improvement effect occurs. However, when the transmission specularity parameter is less than the reflection specularity parameter, the in-plane thermal conductivity of the bi-layer nanofilms becomes lower than that of the suspended nanofilms, that is, the thermal conductivity reduction effect. Additionally, in all the figures above, the interfacial effect is enhanced with the increasing Knudsen number (i.e., the decreasing film thickness); our model can well predict the MC simulation results, verifying the validity of the model.

B. Interface between the disparate materials

In this section, we turn to analyze the thermal transport in the nanofilms with the interface between the disparate materials, which can widely exist in experiments and applications. In practice, the phonon property dissimilarity can mainly be reflected by the MFP ratio between the materials. For example, as for the graphene on the silica substrate,[26] the MFP ratio between graphene and silica can reach about 100. According to Eqs. (8)–(11), the MFP ratio, γ, has been involved in our present model. Here, in order to well clarify the influence of the MFP ratio, we assume that layer "b" is made of a virtual material that holds the identical phonon properties to those with the crystalline silicon (the material of layer "a") except for its intrinsic MFP. Therefore, we can set the intrinsic MFP of layer "a" fixed, and vary that of layer "b" to focus on the influence of MFP ratio on the in-plane

thermal transport within layer "a". We note that our model is actually capable of handling the in-plane thermal transport with an interface between two practical materials, but this can make the analysis process become too trivial to clarify the influence of the MFP ratio.

In Fig. 5, the interface is set completely specular, and the MFP ratios are 0.5, 1, and 1.5, respectively. For the nanofilms with the completely specular interface between the disparate materials (i.e., $\gamma \neq 1$), the in-plane thermal conductivity can differ from that of the suspended nanofilms. As $\gamma = 0.5$, the thermal conductivity reduction effect occurs, whereas $\gamma = 1.5$ can lead to an improvement of the thermal conductivity. For the in-plane thermal transport in the nanofilms, although the completely specular reflection at the interface will not cause the thermal conductivity variation, the phonon transmission through the interface can significantly impact the heat flux distribution, due to the phonon property perturbation near the interface between the disparate materials.[21] In addition, when the transmission specularity parameter equal to the reflection specularity parameter at the interface, the phonon property dissimilarity also causes the thermal conductivity variation. In Fig. 6(a), all the
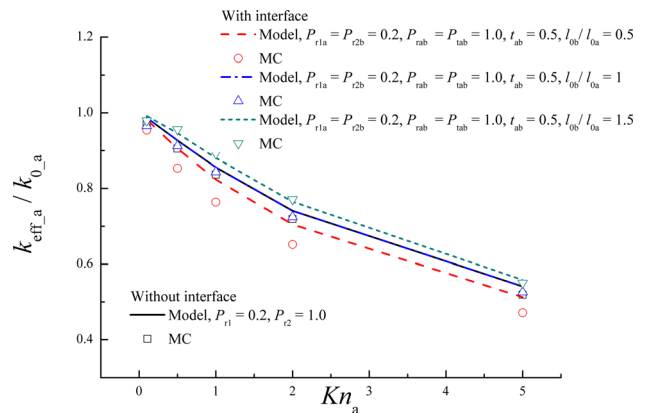

FIG. 5. In-plane thermal conductivity of nanofilms with the completely specular interface between the disparate materials, in comparison to that without the interface. Both the transmission and the reflection specularity parameters at the interface are equal to 1, and the MFP ratios are 0.5, 1, and 1.5, respectively.
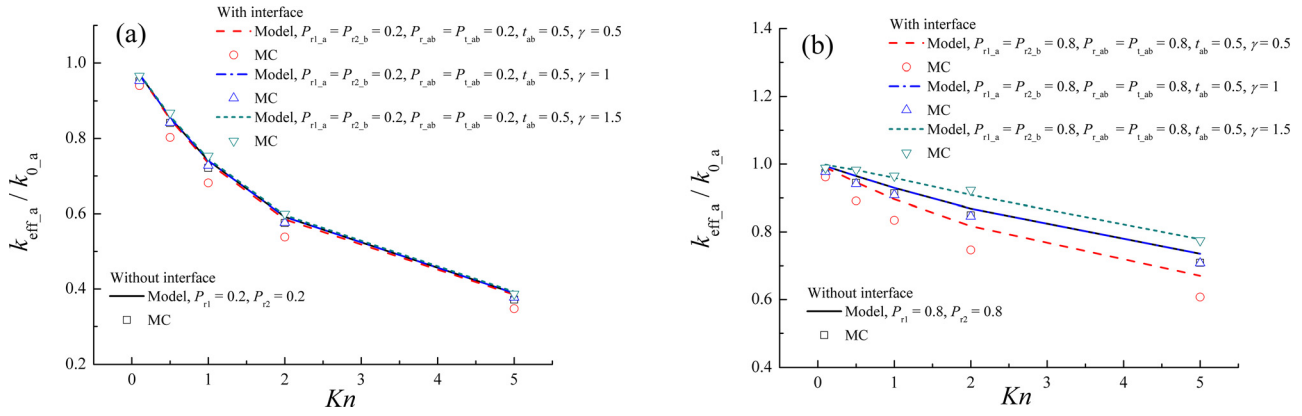
FIG. 6. In-plane thermal conductivity of nanofilms with the partially specular interface between the disparate materials, in comparison to that without the interfacial effect. The transmission specularity parameter is set equal to the reflection specularity parameter at the interface, and the MFP ratios are 0.5, 1, and 1.5, respectively: (a) the specularity parameters are 0.2; (b) the specularity parameters are 0.8.

specular parameters are 0.2, and the phonon transmissivity is 0.5. Although the thermal conductivity variation is not significant, it is also found that as $\gamma = 1.5$, the thermal conductivity improvement effect occurs, whereas $\gamma = 0.5$ can lead to the thermal conductivity reduction effect. In Fig. 6(b), all the specular parameters are increased to 0.8, and the thermal conductivity variation becomes much more significant in this case, indicating that a more specular interface can enhance the influence of phonon property dissimilarity.

In order to further clarify the thermal conductivity variation rule concerning the interfacial effect, the in-plane thermal conductivities of the nanofilms with the partially specular interface were calculated as the functions of the reflection specularity parameter, the transmission specularity parameter, and the phonon transmissivity, respectively. In Fig. 7(a), the Knudsen number is set as 1, the phonon transmissivity is 0.5, and the MFP ratios are 0.5, 1.0, and 1.5, respectively; it was found that the in-plane thermal conductivity increases with the increasing reflection specularity parameter at the interface, despite the MFP ratios. As shown in Fig. 7(b), when the other parameters are given, the in-plane thermal conductivity also increases with the

increasing transmission specularity parameter at the interface, despite the MFP ratios. Therefore, we can confirm that a specular interface can always facilitate the in-plane thermal transport even in the case concerning the phonon property dissimilarity.

In particular, several researchers highlighted the influence of the phonon transmissivity that can involve the influence of the interface adhesion energy.[19] For example, both Yang et al.[27] and Sun et al.[29] concluded that the emergence of the thermal conductivity improvement by the interfacial effect mainly requires a strong interface adhesion energy, that is, a high phonon transmissivity through the interface. As shown in Fig. 8, we also calculated the in-plane thermal conductivity of the nanofilms with the interface as a function of the phonon transmissivity. In Fig. 8(a), the Knudsen number is 1, the transmission specularity parameter is 1, and the reflection specularity parameters are 0.5, and the MFP ratios are 0.5, 1.0, and 1.5, respectively. When the MFP ratio is 1 or 1.5, the thermal conductivity improvement phenomena occurs, and it is enhanced with the increasing phonon transmissivity. This could be the cases Yang et al.[27] and Sun et al.[29] discussed. By contrast, in the case of the MFP ratio less than 1.0 (such as the multi-layer graphene film on a
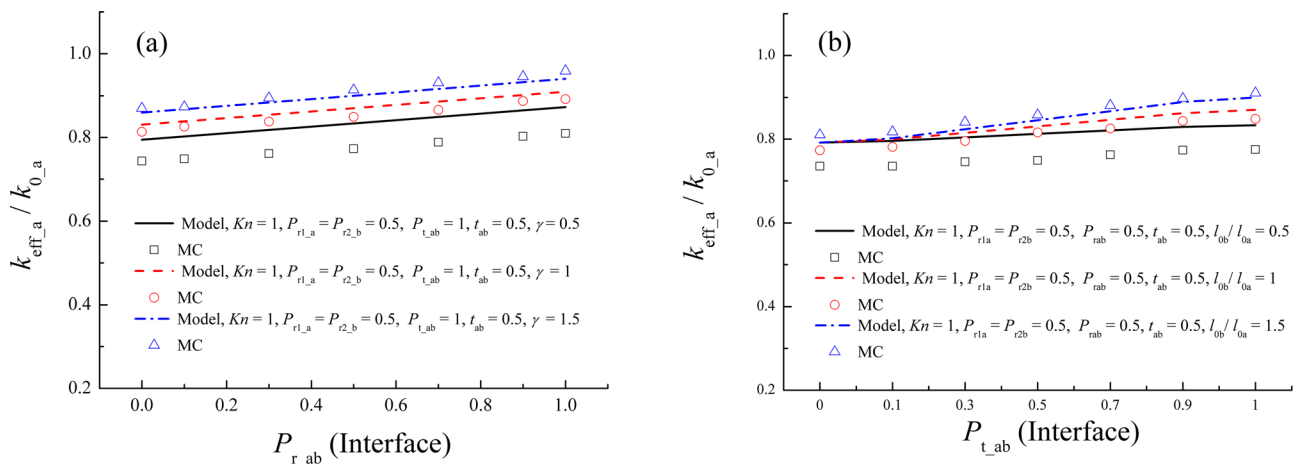

FIG. 7. (a) In-plane thermal conductivity of nanofilms with the partially specular interface as a function of the reflection specularity parameter at the interface; (b) in-plane thermal conductivity of nanofilms with the partially specular interface as a function of the transmission specularity parameter at the interface.
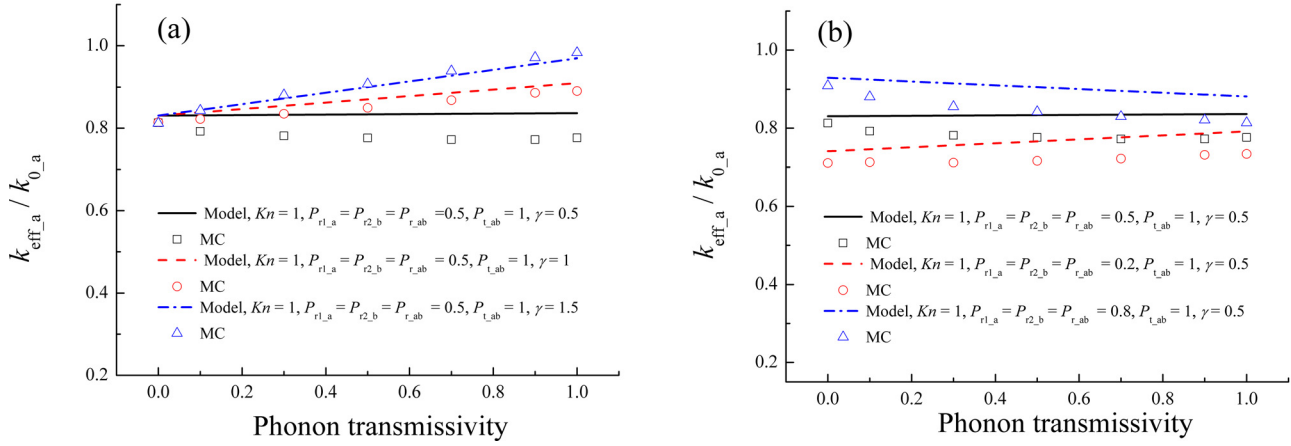
FIG. 8. In-plane thermal conductivity of nanofilms with the partially specular interface as a function of the phonon transmissivity: (a) the transmission specularity parameters are 1, the reflection specularity parameters are 0.5, and the MFP ratios are 0.5, 1.0, and 1.5, respectively; (b) the transmission specularity parameters are 1, the MFP ratios are 0.5, and the reflection specularity parameters are 0.2, 0.5, and 0.8, respectively.

silica substrate[26]), the behavior of the thermal conductivity variation becomes much different. In Fig. 8(b), the MFP ratio is set as 0.5, and the reflection specularity parameters are 0.2, 0.5, and 0.8, respectively. Both the model and the simulations show that when the reflection specularity parameter is equal to 0.2, the thermal conductivity increases with the increasing phonon transmissivity; however, when the reflection specularity parameter is 0.8, the thermal conductivity can decrease with the increasing phonon transmissivity. In this case, there are two competing factors that impact the thermal conductivity. First, the phonons that ballistically transmit through the interface will not undergo diffusive scattering at the interface, which can facilitate the thermal transport. But second, since the MFP ratio is less than 1, the phonon property perturbation near the interface could impede the thermal transport. The coupling strength between the layers is enhanced with the increasing phonon transmissivity. As the reflection specularity parameter is small, the phonons could hold a big possibility to undergo the diffusive scattering once they cannot transmit through the interface. Therefore, the first factor could be dominant when the reflection specularity parameter is small, and the thermal conductivity thus increases with the portion of the phonons that transmit through the interface (i.e., the phonon transmissivity). On the contrary, the second factor can be dominant in the case of a large reflection specularity parameter, and thus, the thermal conductivity decreases with the increasing phonon transmissivity. The conclusion here may be used to explain the controversy between the simulations by Ong et al.[23] and Qiu et al.[24] Their disparity may come from the different interface conditions between the graphene and the silica substrate.

V. CONCLUSIONS

(1) An analytical thermal conductivity model for the in-plane bi-layer nanofilms with the interfacial effect was derived based on the phonon BTE. This model can simultaneously concern the interfacial effect, the phonon property dissimilarity, as well as the disparity between the reflection and the transmission specularity parameters at the interface. Moreover, the phonon MC simulations were used to simulate the phonon transport process in the nanofilms with the interfaces between the identical materials and between the disparate materials. In both the cases, the good agreement between the model and the MC simulations was achieved, indicative of the validity of our model.

(2) In the case of the interface between the identical materials, the emergence of the thermal conductivity variation caused by the interfacial effect requires two conditions: (a) the interface is not completely specular and (b) the transmission specularity parameter is different from the reflection specularity parameter at the interface. In addition, when the transmission specularity parameter is larger than the reflection specularity parameter at the interface, the thermal conductivity improvement effect emerges, whereas the thermal conductivity reduction effect occurs.

(3) In the case of the interface between the disparate materials, the influence of the phonon property dissimilarity was analyzed by varying the MFP ratio, $\gamma = l_{0\omega b}/l_{0\omega a}$. Even when the interface is completely specular or the transmission specularity parameter is identical to the reflection specularity parameter at the interface, the phonon property perturbation near the interface can also cause the thermal conductivity variation. Moreover, it was found that $\gamma > 1$ leads to the thermal conductivity improvement effect, while $\gamma < 1$ corresponds to the thermal conductivity reduction effect.

(4) The two-way tuning of the in-plane thermal transport in the nanofilms was identified by our model and simulations. An interface can reduce or enhance the in-plane thermal conductivity of the nanofilms, depending on the interface conditions and the phonon property dissimilarity at the interface. This can provide a more in-depth understanding about the interfacial effect on the nanoscale thermal transport process. More importantly, an applicable thermal conductivity model was derived and verified in this case, which can be helpful for predicting and manipulating the thermal transport in nanostructures.

ACKNOWLEDGMENTS

[1] K. Mistry, C. Allen, C. Auth, B. Beattie, D. Bergstrom, M. Bost, M. Brazier, M. Buehler, A. Cappellani, R. Chau *et al.*, "A 45 nm logic technology with high-k+metal gate transistors strained silicon, 9 Cu interconnect layers, 193 nm dry patterning, and 100% Pb-free packaging," in *Proceedings of the IEEE International Electron Devices Meeting* (2007), pp. 247–250.

[2] M. Bohr, "The new Era of scaling in an SoC world," in *Proceedings of the IEEE International Solid-State Circuits Conference–Digest of Technical Papers* (2009), pp. 23–28.

[3] A. L. Moore and S. Li, "Emerging challenges and materials for thermal management of electronics," Mater. Today **17**, 163–174 (2014).

[4] D. G. Cahill, P. V. Braun, G. Chen, D. R. Clarke, S. Fan, K. E. Goodson, P. Keblinski, W. P. King, G. D. Mahan, A. Majumdar, H. Maris, S. R. Phillpot, E. Pop, and L. Shi, "Nanoscale thermal transport. II. 2003–2012," Appl. Phys. Rev. **1**, 011305 (2014).

[5] E. Pop, "Energy dissipation and transport in nanoscale devices," Nano Res. **3**, 147–169 (2010).

[6] J. Schleeh, J. Mateos, I. Iniguez-de-la-Torre, N. Wadefalk, P. A. Nilsson, J. Grahn, and A. J. Minnich, "Phonon black-body radiation limit for heat dissipation in electronics," Nat. Mater. **14**, 187–192 (2015).

[7] J. Kaiser, T. Feng, J. Maassen, X. Wang, X. Ruan, and M. Lundstrom, "Thermal transport at the nanoscale: A Fourier's law vs. phonon Boltzmann equation study," J. Appl. Phys. **121**, 044302 (2017).

[8] A. K. Roy, B. L. Farmer, V. Varshney, S. Sihn, J. Lee, and S. Ganguli, "Importance of interfaces in governing thermal transport in composite materials: Modeling and experimental perspectives," ACS Appl. Mater. Interfaces **4**, 545–563 (2012).

[9] P. M. Norris, N. Q. Le, and C. H. Baker, "Tuning phonon transport: From interfaces to nanostructures," J. Heat Transfer **135**, 061604 (2013).

[10] K. Zheng, F. Sun, X. Tian, J. Zhu, Y. Ma, D. Tang, and F. Wang, "Tuning the interfacial thermal conductance between polystyrene and sapphire by controlling the interfacial adhesion," ACS Appl. Mater. Interfaces **7**, 23644–23649 (2015).

[11] B. Liu, J. Baimova, C. D. Reddy, S. V. Dmitriev, W. K. Law, X. Q. Feng, and K. Zhou, "Interface thermal conductance and rectification in hybrid graphene/silicone monolayer," Carbon **79**, 236–244 (2014).

[12] T. English, J. C. Duda, J. L. Smoyer, D. A. Jordan, and P. M. Norris, "Enhancing and tuning phonon transport at vibrationally mismatched solid-solid interfaces," Phys. Rev. B **85**, 035438 (2012).

[13] S. Neogi, J. S. Reparaz, L. F. C. Pereira, B. Graczykowski, M. R. Wagner, M. Sledzinska, A. Shchepetov, M. Prunnila, J. Ahopelto, C. M. Sotomayor-Torres, and D. Donadio, "Tuning thermal transport in ultrathin silicon membranes by surface nanoscale engineering," ACS Nano **9**, 3820–3828 (2014).

[14] J.-H. Zou and B. Y. Cao, "Phonon thermal properties of graphene on H-BN from molecular dynamics simulations," Appl. Phys. Lett. **110**, 103106 (2017).

[15] E. Lee, T. Zhang, T. Yoo, Z. Guo, and T. Luo, "Nanostructures significantly enhance thermal transport across solid interfaces," ACS Appl. Mater. Interfaces **8**, 35505–35512 (2016).

[16] X. Yang, D. Yu, and B.-Y. Cao, "Giant thermal rectification from single-carbon nanotube graphene junction," ACS Appl. Mater. Interfaces **9**, 24078–24084 (2017).

[17] C. Hua, X. Chen, N. K. Ravichandran, and A. J. Minnich, "Experimental metrology to obtain thermal phonon transmission coefficients at solid interfaces," Phys. Rev. B **95**, 205423 (2017).

[18] E. T. Swartz and R. O. Pohl, "Thermal boundary resistance," Rev. Mod. Phys. **61**, 605–668 (1989).

[19] R. Prasher, "Acoutic mismatch model for thermal contact resistance of Van der Waals contacts," App. Phys. Lett. **94**, 041905 (2009).

[20] R. B. Wilson and D. G. Cahill, "Anisotropic failure of Fourier theory in time-domain thermoreflectance experiments," Nat. Commun. **5**, 5075 (2014).

[21] Y.-C. Hua and B.-Y. Cao, "Slip boundary conditions in ballistic–diffusive heat transport in nanostructures," Nanosc. Microsc. Therm. Eng. **21**, 159–176 (2017).

[22] J. H. Seol, I. Jo, A. L. Moore, L. Lindsay, Z. H. Aitken, M. T. Pettes, X. Li, Z. Yao, R. Huang, D. Broido, N. Mingo, R. S. Ruoff, and L. Shi, "Two-dimensional phonon transport in supported graphene," Science **328**, 213–216 (2010).

[23] Z. Ong and E. Pop, "Effect of substrate modes on thermal transport in supported graphene," Phys. Rev. B **84**, 075471 (2011).

[24] B. Qiu and X. Ruan, "Reduction of spectral phonon relaxation times from suspended to supported graphene," Appl. Phys. Lett. **100**, 193101 (2012).

[25] J. Chen, G. Zhang, and B. Li, "Substrate coupling suppresses size dependence of thermal conductivity in supported graphene," Nanoscale **5**, 532 (2013).

[26] M. M. Sadeghi, I. Jo, and L. Shi, "Phonon-interface scattering in multilayer graphene on an amorphous support," PNAS **110**, 16321–16326 (2013).

[27] J. Yang, Y. Yang, S. W. Waltermire, X. Wu, H. Zhang, T. Gutu, Y. Jiang, Y. Chen, A. A. Zinn, R. Prasher, T. T. Xu, and D. Li, "Enhanced and switchable nanoscale thermal conduction due to Van der Waals interfaces," Nat. Nanotechnol. **7**, 91–95 (2012).

[28] Z.-X. Guo, D. Zhang, and X.-G. Gong, "Manipulating thermal conductivity through substrate coupling," Phys. Rev. B **84**, 075470 (2011).

[29] T. Sun, J. Wang, and W. Kang, "Van der Waals interaction-tuned heat transfer in nanostructures," Nanoscale **5**, 128–133 (2013).

[30] R. Su, Z. Yuan, J. Wang, and Z. Zheng, "Enhanced energy transport owing to nonlinear interface interaction," Sci. Rep. **6**, 19628 (2016).

[31] W. Chen, J. Yang, Z. Wei, C. Liu, K. Bi, D. Xu, D. Li, and Y. Chen, "Effects of interfacial roughness on phonon transport in bilayer silicon thin film," Phys. Rev. B **92**, 134113 (2015).

[32] X. Zhang, H. Bao, and M. Hu, "Bilateral substrate effect on the thermal conductivity of two-dimensional silicon," Nanoscale **7**, 6014–6022 (2015).

[33] J. Ziman, *Electrons and Phonons* (Oxford University Press, London, 1961).

[34] X. Wang and B. Huang, "Computational study of in-plane phonon transport in Si thin films," Sci. Rep. **4**, 6399 (2014).

[35] K. Fuchs, "The conductivity of thin metallic films according to the electron theory of metals," Proc. Cambridge Philos. Soc. **34**, 100–108 (1938).

[36] E. H. Sondheimer, "The mean free path of electrons in metals," Adv. Phys. **1**, 1–42 (1952).

[37] J. E. Turney, A. J. H. McGaughey, and C. H. Amon, "In-plane phonon transport in thin films," J. Appl. Phys. **107**, 024317 (2010).

[38] Y.-C. Hua and B.-Y. Cao, "Ballistic-diffusive heat conduction in multiply-constrained nanostructures," Int. J. Therm. Sci. **101**, 126–132 (2016).

[39] A. Malhotra, K. Kothari, and M. Maldovan, "Spatial manipulation of thermal flux in nanoscale films," Nanosc. Microsc. Therm. Eng. **21**, 145–158 (2017).

[40] D. Li and A. J. H. McGaughey, "Phonon dynamics at surfaces and interfaces and its implications in energy transport in nanostructured materials—An opinion paper," Nanosc. Microsc. Therm. Eng. **19**, 166–182 (2015).

[41] L. Yang, Q. Zhang, Z. Cui *et al.*, "Ballistic phonon penetration depth in amorphous silicon dioxide," Nano Lett. **17**, 7218–7225 (2017).

[42] Y.-C. Hua and B.-Y. Cao, "Phonon ballistic-diffusive heat conduction in silicon nanofilms by Monte Carlo simulations," Int. J. Heat Mass Transfer **78**, 755–759 (2014).

[43] J. P. M. Peŕaud and N. G. Hadjiconstantinou, "An alternative approach to efficient simulation of micro/nanoscale phonon transport," Appl. Phys. Lett. **101**, 153114 (2012).

[44] Y.-C. Hua and B.-Y. Cao, "An efficient two-step Monte Carlo method for heat conduction in nanostructures," J. Comput. Phys. **342**, 253–266 (2017).

[45] Y.-C. Hua and B.-Y. Cao, "Cross-plane heat conduction in nanoporous silicon thin films by phonon Boltzmann transport equation and Monte Carlo simulations," Appl. Therm. Eng. **111**, 1401–1408 (2017).

[46] K. D. Parrish, J. R. Abel, A. Jain, J. A. Malen, and A. J. H. McGaughey, "Phonon-boundary scattering in nanoporous silicon films: Comparison of Monte Carlo techniques," J. Appl. Phys. **122**, 125101 (2017).

[47] G. Chen, "Thermal conductivity and ballistic-phonon transport in the cross-plane direction of superlattices," Phys. Rev. B **57**, 14958–14973 (1998).